Structural aspects of lithium insertion in transition metal oxide electrodes

H. Berg [a], Ö. Bergström [a], T. Gustafsson [a], E.M. Kelder [b], J.O. Thomas [a,*]

[a] *Institute of Chemistry, Uppsala University, Box 531, 751 21 Uppsala, Sweden*
[b] *Delft University of Technology, PO Box 5054, 2600 GA Delft, The Netherlands*

Abstract

There is a considerable lack of detailed information on the structure of lithiated phases of popular-consensus positive electrode materials for lithium/polymer and lithium-ion/polymer batteries. Having illustrated this phenomenon for the specific cases of $LiMn_2O_4$ and V_6O_{13}, some suggestions are made to present the problem in a more general context. The need for single-crystal diffraction studies is indicated. © 1997 Published by Elsevier Science S.A.

1. Introduction

Lithium-ion/polymer and lithium/polymer batteries satisfy many of the performance requirements imposed by the portable electronics industry. A critical feature of these batteries is the composite cathode, comprising an active transition metal oxide (TMO), carbon in any form to provide electronic conductivity, and a small amount of binder [1].

A more complete understanding of charge/discharge mechanisms in these batteries thus necessitates the study of lithiation processes in TMOs at atomic level. An essential basis for such studies, however, is a precise knowledge of the crystal structures of the various lithiated phases involved. Remarkably, this type of information is often lacking, with the implication that discussion of the relative advantages of different positive-electrode materials must necessarily be highly tenuous.

We present this problem from the viewpoint of two popular consensus TMO materials: $LiMn_2O_4$ and V_6O_{13}. By analysing some relevant structural issues on these compounds, it emerges that certain changes in strategy may provide a more detailed structural information in a more general context.

1.1. $Li_{1+x}Mn_{2-x}O_4$

$LiMn_2O_4$ has the spinel structure (space group: $Fd3m$) in which the oxygen atoms form a cubic close-packed array: the Mn ions located at the octahedral sites and the Li ions at the
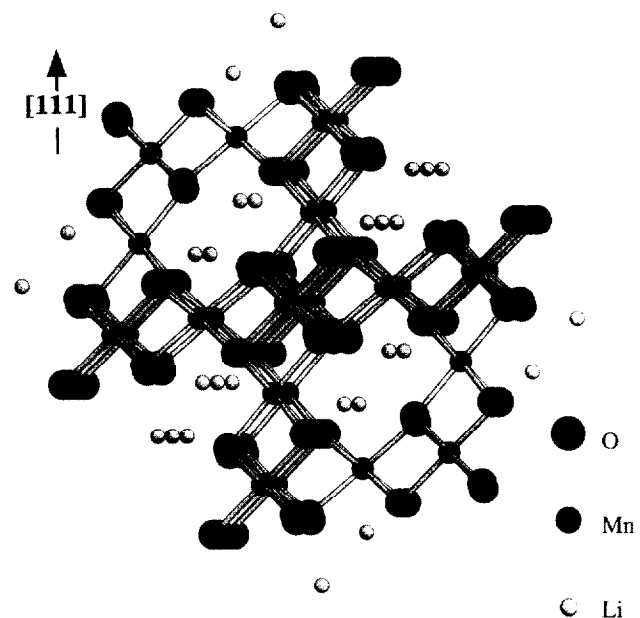
Fig. 1. Structure of stoichiometric $LiMn_2O_4$.

tetrahedral sites (Fig. 1). A Jahn–Teller distortion may cause a cubic-to-tetragonal phase transition when the average valence of the Mn ions falls below + 3.5. This occurs at the 3 V plateau, i.e. when Li is inserted into the $Li_1Mn_2O_4$ spinel, and is accompanied by a loss of Li storage capacity. An underlying theme of current work on the $LiMn_2O_4$ system is therefore to suppress this Jahn–Teller distortion, and thereby to increase the effective Li capacity. One way to stabilize $LiMn_2O_4$ has been to incorporate defects into the Mn–O lat-

* Corresponding author.
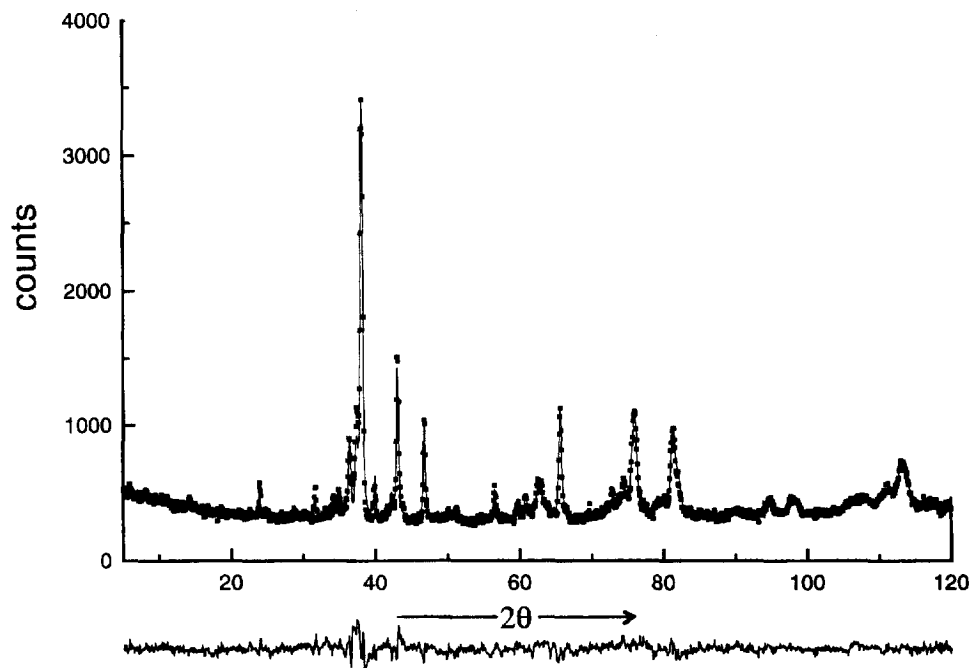
Fig. 2. Rietveld fit of neutron powder diffraction data for chemically lithiated V_6O_{13}.

tice by synthesizing stoichiometric spinels with the general formula $Li_{1+x}Mn_{2-x}O_4$, $0 < x < 1/3$ [2], thereby increasing the Li/Mn ratio (and thus minimizing the number of Mn ions which can contribute to the Jahn–Teller distortion). It has generally been assumed that the 'extra' Li substitute into the structure at the octahedral Mn vacancies which are created.

1.2. V_6O_{13}

Many proposals of phases formed on inserting Li into the V_6O_{13} structure are found in the litterature; sets of x values in $Li_xV_6O_{13}$ such as 0.5, 1.5, 3.0, 6.0 and 1.0, 4.0, 8.0 are are given in Refs. [3,4]. These results were derived from a combination of powder X-ray diffraction (XRD) and electrochemical studies.

Much of our earlier work to study Li-insertion mechanisms in V_6O_{13} involved in situ XRD in transmission mode on working cells [5]. An intrinsic deficiency of this type of study, however, is its inability to distinguish features associated with a single V_6O_{13} particle from those related to the composite nature of the cathode. In situ powder XRD data are often inadequate in providing more than qualitative information on structural changes in the battery during cycling. Even ex situ XRD and neutron diffraction (ND) studies of chemically lithiated $Li_xV_6O_{13}$ powders have been unsuccessful in solving their crystal structure. Despite an apparently successful Rietveld refinement of the ND data (Fig. 2), the resulting Li positions corresponded to unrealistic Li-coordination and much foreshortened Li–O distances. Powder XRD techniques generally seem unable to resolve structural subtleties in the lithiation process. We turn therefore to the use of single-crystal XRD techniques. A single-crystal data set contains between ten and a hundred times as many significant

reflections as a powder data set, resulting in an improved resolution.

2. Experimental

2.1. $Li_{1+x}Mn_{2-x}O_4$

Efforts to improve the potential Li storage capacity of $LiMn_2O_4$ spinel led us to the investigation of Li-rich phases. Powders of the stoichiometric spinel phase $Li_{1+x}Mn_{2-x}O_4$ were synthesized in a two-stage process. Mixtures of $LiOH \cdot H_2O$ and manganese acetate with different Li/Mn ratios were dissolved by stirring at about 120°C together with a small amount of water. This precursor material was then calcined by heating in air at 60 °C for 10 h, and cooling slowly to room temperature. After calcination, the powder was ground at 600°C for 5 h [6]. The Li/Mn ratio was 0.75, corresponding to a stoichiometric spinel phase $Li_{1+x}Mn_{2-x}O_4$ with an x value of 2/7.

Neutron powder diffraction data were then collected at 22°C at the R2 medium-flux reactor in Studsvik, Sweden, and XRD data were obtained using a STOE & CIE GmbH STADI position-sensitive detector (PSD) diffractometer with Cu $K\alpha_1$ radiation.

2.2. V_6O_{13}

2.2.1. Single-crystal synthesis

Crystallographically pure V_6O_{13} powder was obtained by thermal decomposition of ammonium vanadate, as described in Ref. [7]. This powder was mixed with a transport agent $TeCl_4$ ($V_6O_{13}/TeCl_4$ mass ratio 20/1), and the mixture used

as the starting material for growing larger single crystals of V_6O_{13} by chemical vapour transport (CVT) in evacuated silica tubes [8].

2.2.2. Electrochemical lithiation

Crystals with a maximum dimension of 0.1 mm were screened on a single-crystal XRD diffractometer. These were incorporated individually into the composite cathode of a cell (anode: Li foil; polymer gel electrolyte with $LiAsF_6$ salt; composite cathode: 80 wt.% V_6O_{13}, 15 wt.% Shawinigan black and 5 wt.% ethylenepropylenediene polymer (EPDM) binder). The cell was discharged from an initial 3.0 V versus Li/Li^+ down to 2.65 V by an electrochemical voltage spectroscopy technique (EVS) [9]. The potential was stepped by 10 mV, when the current density declined to 0.2 $\mu A/cm^2$. The 2.65 V potential corresponds to the first lithiated phase of V_6O_{13} under discharge [5] (Fig. 3). To promote the kinetics of the lithiation process, the cell was maintained at this voltage in a sand-bath kept at 50 °C for 42 days (Fig. 4). The
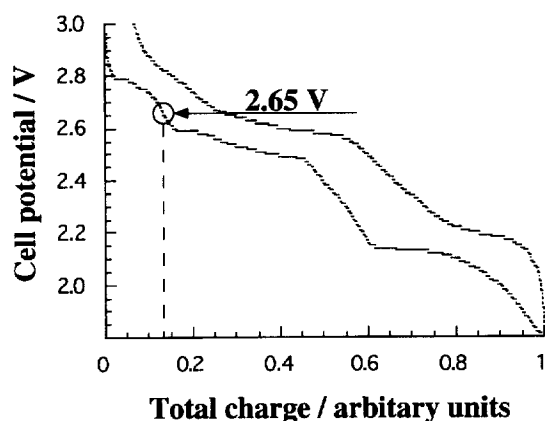
Fig. 3. EVS cycling curve for a cell containing V_6O_{13}. The arrow indicates the voltage vs. Li/Li^+ at which the structure of the first lithiated phase was studied.
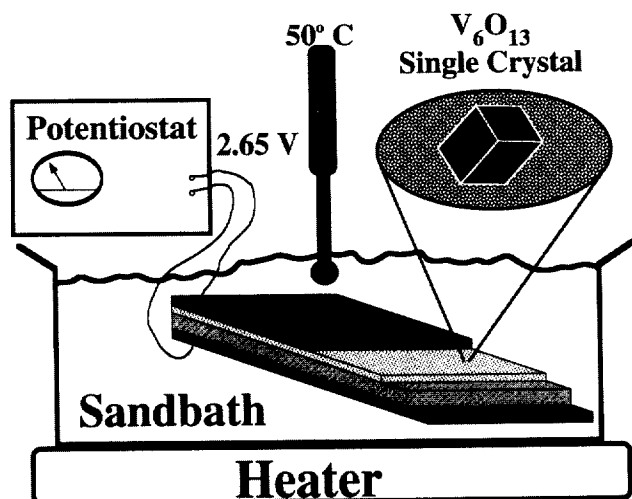
Fig. 4. Experimental set-up for the electrochemical lithiation of single-crystal V_6O_{13}.

cell was dismantled inside an argon-filled glove box (< 1 ppm O_2 and < 1 ppm H_2O) fitted with a microscope, and the lithiated single crystal mounted on a goniometer head. The crystal was given a protective layer of polystyrene before it was removed from the glove box.

2.2.3. Single-crystal XRD

A complete single-crystal data set comprising 5730 measured (2876 independent) reflections was collected on a STOE & CIE 4-circle automatic X-ray diffractometer. Intensity decay, absorption and anisotropic extinction corrections were applied to the data. The Li positions were determined from a difference Fourier synthesis, starting with atomic coordinates known for V_6O_{13} [10].

3. Results and discussion

3.1. $Li_{1+x}Mn_{2-x}O_4$

The ND profile has been refined by the Rietveld method using the non-Li atoms of the cubic $LiMn_2O_4$ spinel structure as a starting point. Again (as in the case of $Li_xV_6O_{13}$, see Fig. 2), despite a remarkably good fit to the experimental data (Fig. 5), one peak could not be explained. This indicated the presence of an impurity phase in our synthesized powder. Thorough analysis revealed a two-phase mixture of $Li_{1+x}Mn_{2-x}O_4$ and Li_2MnO_3; the extra peaks from Li_2MnO_3 are seen clearly by XRD (see also Ref. [11]). A subsequent two-phase Rietveld refinement gave a composition of 90 wt.% $Li_{1+x}Mn_{2-x}O_4 + 10$ wt.% Li_2MnO_3, and a refined x value of 0.16(2), with the 'extra' 0.16 Li occupying a second octahedral site (16c), different from that occupied by the Mn ions (16d) (See Table Table 1). Some Li may also occupy the Mn site. This will be discussed later in a more detailed paper. Clearly, instead of an expected x value of 2/7, the second phase 'steals' Li from the starting materials, resulting in a lower x value. The refinement also confirms a corresponding 5.2% depletion at the Mn sites. The phenomenon that the extra Li does not replace the Mn ions, as earlier reported [2], means that we must change our view of Li insertion and extraction mechanisms in the stoichiometric Mn spinel phase.

From a point of view of battery application, the impurity phase (Li_2MnO_3) is electrochemically inactive, and therefore a source of unwanted capacity loss. Efforts during the synthesis process must therefore be focused on achieving phase-pure $Li_{1+x}Mn_{2-x}O_4$; the relevant region of the phase diagram is shown in Fig. 6. It is clear that diffraction may easily fail to detect the presence of the Li_2MnO_3 impurity: its strong reflections overlap almost completely those from the stoichiometric spinel structure, compare Figs. 1 and 7; the two structures are very similar, d_{111} for the spinel phase (4.721 Å) being almost the same as d_{002} for Li_2MnO_3 (4.730 Å).
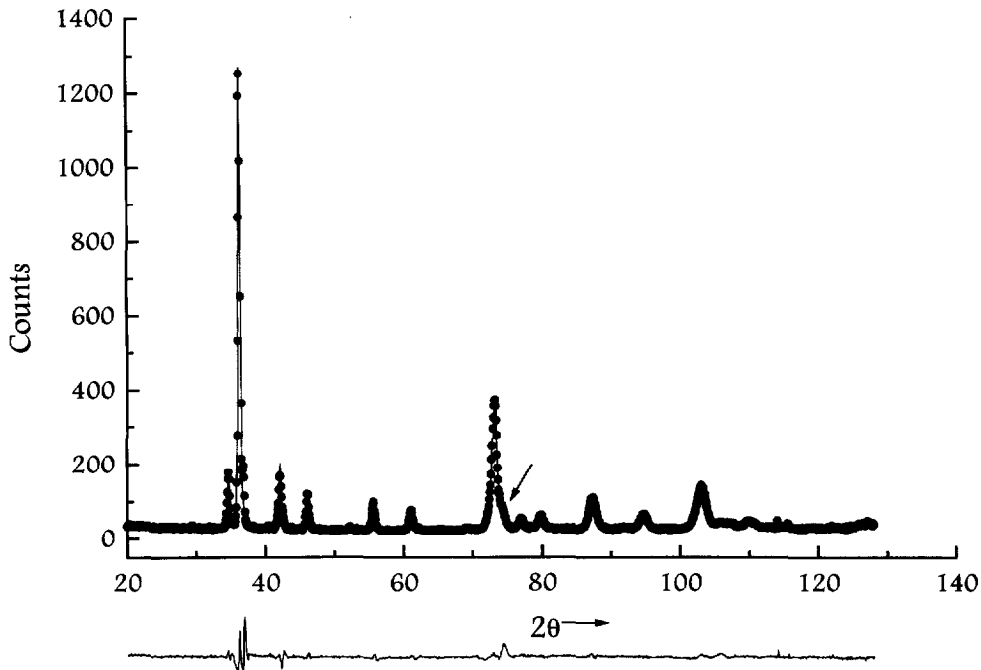
Fig. 5. Rietveld fit of neutron powder diffraction data for a mixture of $Li_{1+x}Mn_{2-x}O_4 + Li_2MnO_3$ to a single-phase model.

Table 1
The structure of $Li_{1+x}Mn_{2-x}O_4$ ($x = 0.16(2)$), as determined from neutron diffraction data

Atom	Site	x	y	z	$B_{iso}/Å^2$ [a]	Site occupancy (%)
Li (1)	8a	0.125	0.125	0.125	1.156	100
Li (2)	16c	0	0	0	1.156	8.43(1)
Mn	16d	0.5	0.5	0.5	0.525	94.82(1) [b]
O	32e	0.2637(1)	0.2637(1)	0.2637(1)	0.925	100

$a = 8.1778(6)$ Å; $R_p = 6.35\%$, $R_{wp} = 8.47\%$, $R_{Bragg} = 5.54\%$.
[a] Values taken from unpublished data.
[b] Site can also contain lithium.
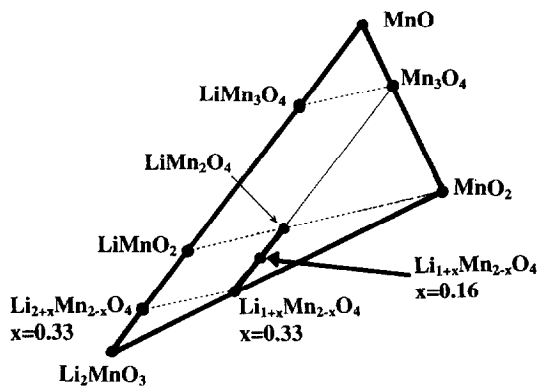
Fig. 6. Region of the phase diagram around $Li_{1+x}Mn_{2-x}O_4$.

3.2. $Li_2V_6O_{13}$

The space group of the $Li_2V_6O_{13}$ structure [12] and the unlithiated V_6O_{13} structure [11] is $C2/m$. The major effect of lithiation is a 7.6% expansion of the c-axis, which is the stacking direction in the structure (Fig. 8(a)). The Li ions are located between layers of the V_6O_{13} structure, with an
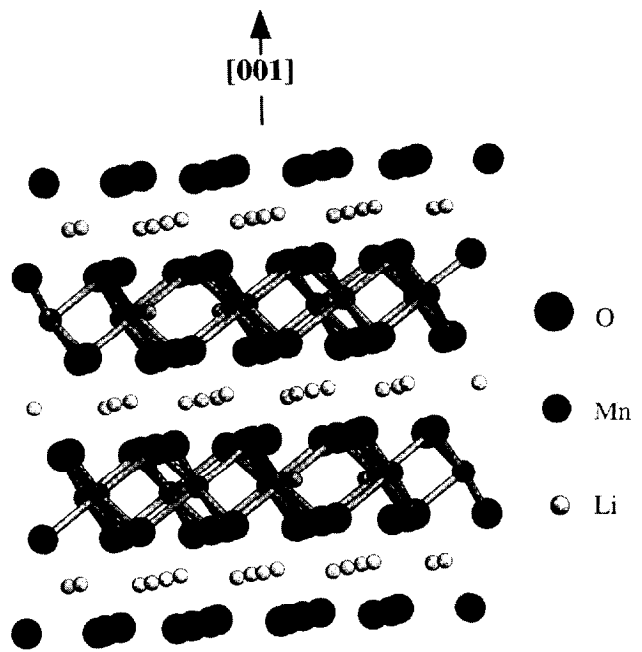
Fig. 7. Structure of Li_2MnO_3 viewed approximately along its c-axis.
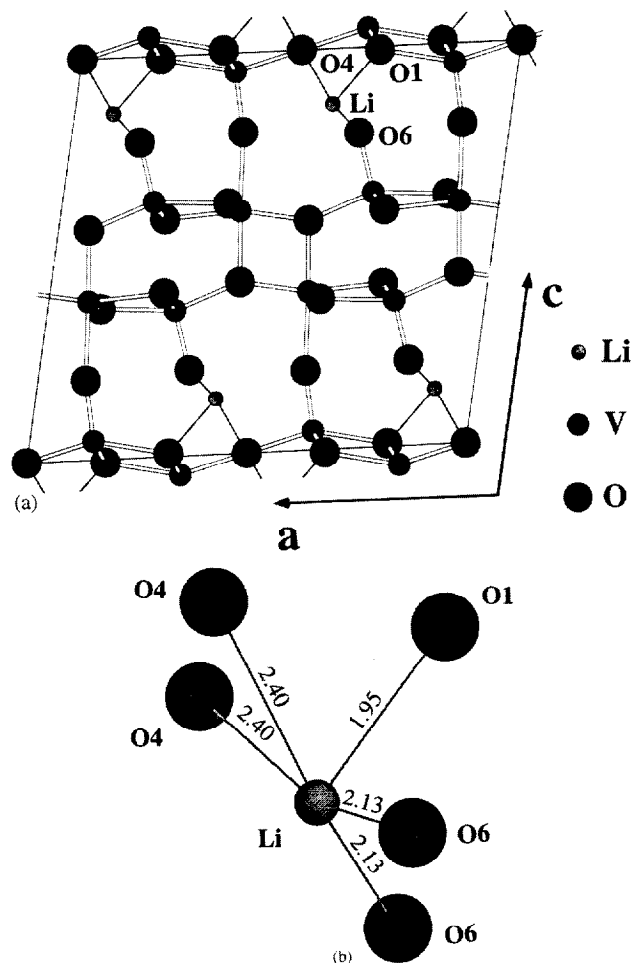
Fig. 8. (a) Structure of $Li_2V_6O_{13}$ viewed along its b-axis; (b) showing the oxygen coordination around the lithium ion.

Table 2
Structure of $Li_2V_6O_{13}$ as determined from single-crystal X-ray diffraction data

Atom	x	y	z	B_{eq} (Å^2) [a]
Li	0.08553(25)	0	0.13685(25)	3.05
V(1)	0.35436(1)	0	0.04678(1)	0.43
V(2)	0.40922(1)	0	0.39463(1)	0.44
V(3)	0.70902(1)	0	0.36350(1)	0.45
O(1)	0.18027(5)	0	0.00799(5)	0.59
O(2)	0.87936(5)	0	0.37472(5)	0.60
O(3)	0.23984(5)	0	0.40683(6)	0.76
O(4)	0.5	0	0.5	0.89
O(5)	0.39003(6)	0	0.19866(5)	0.92
O(6)	0.65783(6)	0	0.21349(6)	1.04
O(7)	0.56855(5)	0	0.42661(5)	0.56

[a] $B_{eq} = (4/3)\Sigma_i\Sigma_j\beta_{ij}a_ia_j$.

interesting five-fold coordination to oxygen atoms in a tetragonal pyramid arrangement (Fig. 8(b)).

Refinement of 71 parameters (including anisotropic temperature factors) gave a final weighted R value of 5.5% (Table 2). The Li position (a $4i$-site) refined to full occupancy is consistent with the composition $Li_2V_6O_{13}$. This is somewhat in conflict with earlier studies: such a high Li

content has not been reported for the lithiated phase at 2.65 V. The reasons could be the following.

(i) Typical V_6O_{13} particles in the cathode have a $\sim 10^6$ times larger volume than the single crystal used in the structural study. However, the use of long equilibration times and small voltage steps should result in the same lithiated phase.

(ii) The effect of using an elevated temperature (50 °C) has not been thoroughly investigated. That the discharge curve is temperature dependent could explain the differences compared with the results of the room temperature powder studies [3,4].

We may also note that the large unit-cell expansion on lithiation could underly the intial capacity loss observed in cells containing V_6O_{13}. Cracking has also been observed in larger V_6O_{13} particles; both expansion and cracking can cause particles to lose contact with the polymer electrolyte or with the electronically conducting carbon powder.

4. Conclusions

A number of important structural features relevant to the $LiMn_2O_4$ and V_6O_{13} systems have emerged:

1. Efforts to synthesize Li-rich $Li_{1+x}Mn_{2-x}O_4$ can easily result in the presence of the monoclinic impurity Li_2MnO_3. The two cells are closely similar, making it difficult to be detected in small quantities.
2. The 'extra' Li in $Li_{1+x}Mn_{2-x}O_4$ substitutes primarily into the octahedral 16c-site at (0,0,0) in the cubic spinel structure. Some Li may also enter the octahedral 16d Mn site.
3. Powder diffraction methods (both in and ex situ) can be unsuccessful in giving the correct $Li_xV_6O_{13}$ structures; significantly more sensitive single-crystal XRD data may well be mandatory if these structures are to be solved.
4. The first Li insertion phase of V_6O_{13}, as determined by an accurate single-crystal XRD study, is $Li_2V_6O_{13}$.

In a more general context, although in situ XRD data certainly has an important rôle in the understanding of Li insertion and de-insertion mechanisms in a qualitative way, it may be inadequate in providing detailed information on the structure of the lithiated phases, especially in view of the low X-ray scattering power of Li^+ ions; it may well be necessary to turn to single-crystal XRD in combination with powder ND to obtain this information.

References

[1] B. Scrosati, Applications of Electroactive Polymers, Chapman and Hall, London, 1993, Ch. 6.

[2] R.J. Gummow, A. de Kock and M.M. Thackeray, *Solid State Ionics*, *69* (1994) 59.

[3] C. Lampe-Önnerud, P. Nordblad and J.O. Thomas, *Solid State Ionics*, *81* (1995) 189.

[4] K. West, B. Zachau-Christianssen, T. Jacobsen and S. Atlung, *J. Power Sources*, *14* (1985) 235.

[5] T. Gustafsson, J.O. Thomas, R. Koksbang and C.G. Farrington, *Electrochim. Acta*, *37* (1992) 1639.

[6] I. Chen, X. Huang, E.M. Kelder and J. Schoonman, *Solid State Ionics*, *76* (1995) 91.

[7] C. Lampe-Önnerud and J.O. Thomas, *Eur. J. Solid State Inorg. Chem.*, *32* (1995) 293.

[8] M. Saeki, N. Kimizuka, M. Ishii, I. Kawada, M. Nakano, A. Ichinose and M. Nakahira, *J. Cryst. Growth*, *18* (1973) 101.

[9] A.H. Thomson, *Phys. Rev. Lett.*, *23*(1978) 1511.

[10] K.A. Wilhelmi, K. Waltersson and L. Kihlborg, *Acta Chem. Scand.*, *25* (1971) 2675.

[11] Y. Gao and J.R. Dahn, *J. Electrochem. Soc.*, *143* (1996) 100.

[12] Ö. Bergström, T. Gustafsson and J.O. Thomas, *Acta Crystallogr. C*, *25* (1997) 528.